

# Allowable number of plasmons in nanoparticle

*I. A. Fedorov<sup>a,b</sup>, V. M. Parfenyev<sup>a,c1)</sup>, S. S. Vergeles<sup>a,c</sup>, G. T. Tartakovskiy<sup>d</sup>, A. K. Sarychev<sup>e</sup>*

*<sup>a</sup>Moscow Institute of Physics and Technology, 141700 Dolgoprudny, Russia*

*<sup>b</sup>Russian Quantum Center, 143025 Moscow, Russia*

*<sup>c</sup>Landau Institute for Theoretical Physics of the RAS, 117940 Moscow, Russia*

*<sup>d</sup>Advanced Systems and Technologies, 92018 Irvine, CA*

*<sup>e</sup>Institute for Theoretical and Applied Electromagnetics of the RAS, 125412 Moscow, Russia*

Submitted 2 September 2014

Resubmitted 17 September 2014

We address thermal and strength phenomena occurring in metal nanoparticles due to excitation of surface plasmons. The temperature of the nanoparticle is found as a function of the plasmon population, allowing for the Kapitza heat boundary resistance and temperature dependencies of the host dielectric heat conductivity and the metal electrical conductivity. The latter is shown to result in the positive thermal feedback which leads to appearance of the maximum possible number of plasmon quanta in the steady-state regime. In the pulsed regime the number of plasmon quanta is shown to be restricted from above also by the ponderomotive forces, which tend to deform the nanoparticle. Obtained results provide instruments for the heat and strength management in the plasmonic engineering.

DOI: 10.7868/S0370274X14200107

A decade ago the enhancement of surface plasmons in metal nanoparticles (NPs) by optical gain was predicted theoretically [1–3] and demonstrated in the experiments [4, 5]. These results opened venue of construction the loss-free optical metamaterials [6], subwavelength waveguides [7], nanosensors [8], etc. Recently a lot of work was focused on nano-sized sources of light, see, e.g., [9]. A metal NP embedded in the dielectric environment is a unit cell of almost all these applications. Extensive heat generation near the plasmonic resonance of the metal NPs is a limiting factor in a lot of experiments [9]. The heat management will increase its urgency as the plasmonic technology will mature and find a widespread commercial use. Here we present a basic theoretical ground for analysis of the thermal and the strength phenomena. The latter is produced by the ponderomotive forces and can be a limitation factor for the plasmon population as well.

The surface plasmon has two channels of decay. Firstly, the plasmonic oscillator is coupled to the far field modes. This provides the possibility for the plasmon to release its energy by emitting a photon, without contribution to the temperature of the system. Secondly, the electromechanical energy of the plasmon is converted to the heating of the particle. In the letter, we consider

the heat processes in NP when the plasmon mode is excited in continuous and pulsed regimes and obtain the temperature of the NP versus the number of plasmon quanta. We show, that the NP can readily heat up to the melting point, and thus the admissible plasmon population is limited. We also consider another limiting factor caused by ponderomotive force, which tries to deform the NP mechanically. The force is proportional to the energy density and it is huge due to the nanoscale mode confinement.

Let us first consider the heat transfer from the NP when the plasmon is excited externally in the continuous wave regime (CW). We assume the simplest experimental arrangement, when the spherical NP of radius  $a$  is placed inside the massive bulk of the host dielectric, and the fundamental plasmon mode of frequency  $\omega$  is permanently populated by  $n$  quanta. For simplicity we disregard possible photothermal effect presented in the pumping process and focus on the heat generation due to plasmon decay. Power losses  $P$  of plasmon mode are determined by the  $Q$ -factor and can be split in heat and radiation losses:

$$\frac{n\hbar\omega^2}{Q} = n\hbar\omega(\gamma_{\text{heat}} + \gamma_{\text{rad}}) = P_{\text{heat}} + P_{\text{rad}}, \quad (1)$$

where  $\gamma$ 's are decay rates. In most cases of interest,  $P_{\text{rad}}$  is the dipole radiation and thus  $\gamma_{\text{rad}}/\gamma_{\text{heat}} \propto (ka)^3/\varepsilon_m''$

---

<sup>1)</sup>e-mail: parfenius@gmail.com

[10], where  $k = \sqrt{\epsilon_d} \omega / c$  is the corresponding wave vector,  $\epsilon_d$  is the dielectric permittivity of the surrounding medium, and  $\epsilon_m''$  is the imaginary part of the dielectric permittivity of the NP. For gold NPs in the optical range dipole radiation comes into play at the radius of  $a \sim 20$  nm. Below this size,  $\gamma_{\text{rad}} \ll \gamma_{\text{heat}}$ , and  $Q \simeq \omega / \gamma_{\text{heat}}$ . In the case of multipolar modes (so called dark modes) the evaluation is valid for wider range of sizes, due to the modes are poorly coupled to the far field, and ratio  $\omega / \gamma_{\text{heat}}$  is nearly the same for different modes [11].

The heat transfer from the NP occurs both through the diffusive and ballistic mechanisms. We shall take into account only the former, which leads to the upper estimation of the real heat flux, see [12, 13]. Then, the temperature profile is determined by the heat conductivity  $\chi$  of the surrounding medium and the Kapitza conductance  $h$  of the NP interface [14], which is relevant at nanoscales [15]. We start with the simplest model, when  $\chi$  is assumed to be temperature independent. Then, the temperature difference between the NP surface ( $T$ ) and infinity ( $T_0$ ), caused by the heat generation power  $P_{\text{heat}}$ , is found via the standard Fourier law:

$$\delta T = T - T_0 = \frac{n\hbar\omega\gamma_{\text{heat}}}{4\pi a^2 h_{\text{NP}}}, \quad (2)$$

where  $1/h_{\text{NP}} = 1/h + a/\chi$ . Temperature inside the NP can be regarded as uniform since the thermal conductivity of the metal is much larger than that of the dielectric host. To establish the NP temperature  $T$  from (2), we take into account the temperature dependence of the plasmon decay rate  $\gamma_{\text{heat}}(T)$ . It can be approximated by linear dependence, which stems mainly from the electron-phonon scattering:

$$\hbar\gamma_{\text{heat}}(T) = \alpha + \beta T. \quad (3)$$

Considering gold as the most studied plasmonic metal and using data from [16–19] we adopt  $\beta = 10^{-4}$  eV/K and  $\alpha = 0.07$  eV for  $\hbar\omega = 1.9$  eV. Approximation (3) is valid from  $\sim 50$  K up to  $\sim 1100$  K, where premelting or melting of gold starts [18, 20].

The temperature of the NP as a function of the plasmon population in the steady state is shown in the Fig. 1. The red line corresponds to the toy model, where we neglect the Kapitza heat resistance  $h \rightarrow \infty$  and assume  $\chi = 1.4$  W/(m·K) as for vitreous silica at standard conditions. Its superlinear behavior is the result of the temperature-dependent  $\gamma_{\text{heat}}$  (3), which realizes a thermal positive feedback. This is expected to take place in other metals as well, though the dependence can be more complicated, as it is found for silver [21].

Note, that the temperature tends to infinity at some critical plasmon number

$$n_{\text{crit}} = \frac{4\pi a^2 h_{\text{NP}}}{\omega\beta}, \quad (4)$$

which gives the upper limit of the plasmonic population per NP.

Actual the value of the heat conductance  $\chi$  is seen to depend on the temperature for the typical host materials. In the following, we consider the cases of vitreous silica and crystalline quartz, adopting  $\chi(T)$  from papers [22, 23]. Numerical solution of the resulting heat balance equation is shown as dashed and dot-dashed lines, which stand for the Kapitza conductance of  $h = \infty$  and  $h = 10^8$  W/(m<sup>2</sup>·K). The latter value is taken from [14] in absence of direct experimental data. The real dependencies are expected to lie between these pairs of reference lines.

For vitreous silica,  $\chi$  increases with temperature [22] and thereby suppresses the positive thermal feedback, while the crystalline quartz behaves oppositely [23], see dashed lines in the Fig. 1. In the crystalline case the dependence  $\chi(T)$  can be approximated as  $\chi_0\Theta/T$  (where  $\chi_0$  and  $\Theta$  are constants, see, e.g., [23]). In that case the heat equation can be solved analytically, under the assumption that  $h \rightarrow \infty$ . One arrives to the same expression (4) for the critical plasmon number, where the heat conductivity  $\chi$  should be taken at the temperature  $T^*$ , which satisfies the transcendental equation  $1 + \alpha/(\beta T^*) = \log(T^*/T)$ .

Note that the temperature divergence at some critical point remains valid for most of the calculations with real  $\chi(T)$ , though the value of  $n_{\text{crit}}$  may shift. As such, existence of  $n_{\text{crit}}$  (4) is not an artifact of our toy model, but relevant practical prediction. Direct experimental examination of this phenomenon would be of great importance for the future study. More practically important, though, may be threshold of achieving some specific temperature, say the metal melting point  $T_{\text{melt}}$ , which may cause destruction of the plasmonic system. As appears from the Fig. 1, for different conditions this is expected to occur at the plasmon populations ranging from  $n_{\text{melt}} \sim 1$  up to  $\sim 6$ . Note that sometimes  $n_{\text{melt}}$  can be successfully estimated in the most naive way, with  $h \rightarrow \infty$  and  $\gamma_{\text{heat}}$  taken at room temperature, see black line in the Fig. 1.

Above, we have disregarded the thermal radiation power  $P_T$ . To estimate it note, that Stefan–Boltzmann law is not applicable in the case due to the skin layer depth is greater than the NP size and  $P_T$  is produced by the dipole radiation rate [24]. Using fluctuation-dissipation theorem (see e.g. [25]), we obtain  $P_T \sim$

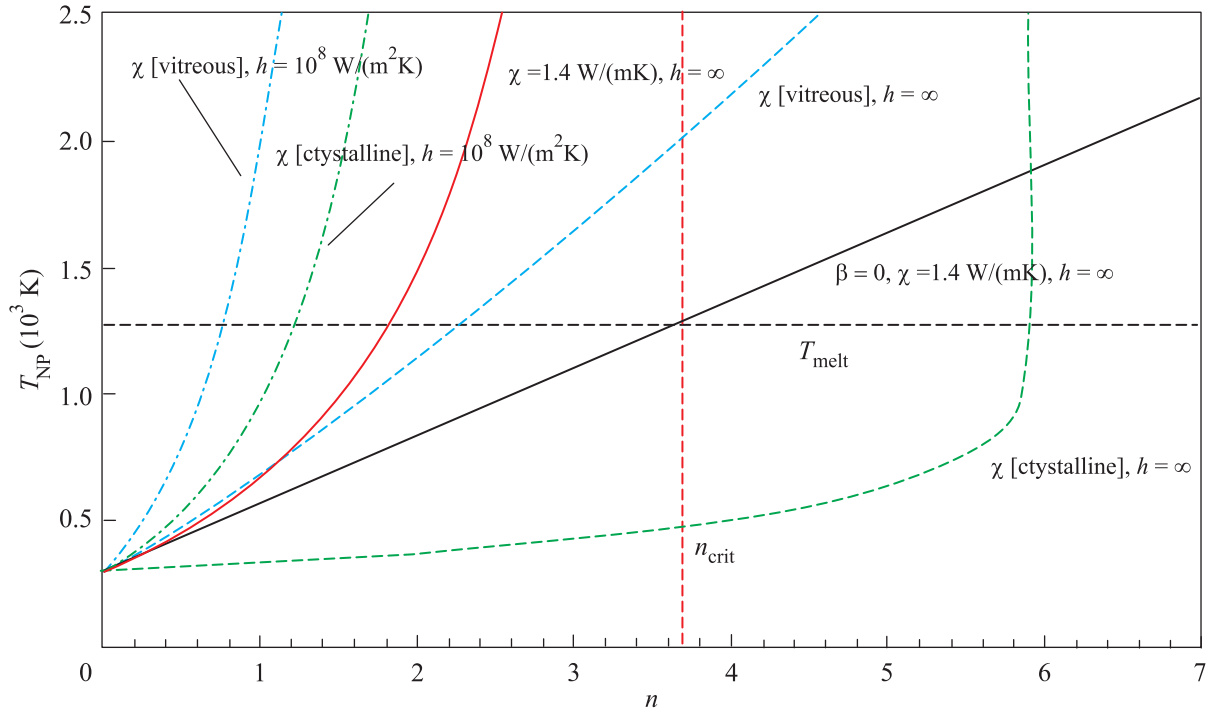


Fig. 1. (Color online) The steady-state temperature of the NP versus the number of plasmons. Parameters used:  $a = 10 \text{ nm}$ ,  $\hbar\omega = 1.9 \text{ eV}$ , and  $T_0 = 300 \text{ K}$ . The gold melting point is taken to be  $T_{\text{melt}} \approx 1270 \text{ K}$  [20]

$\sim T^5 \alpha''/\hbar^4 c^3$ , where  $\alpha''$  is the imaginary part of the NP electrical polarizability at frequency  $\omega_T = T/\hbar$ . The upper estimation for it is  $a^3$  out of resonance, thus we arrive to  $P_T \sim (\omega_T/c)^3 T^2/\hbar$  that is negligible compared to total power losses  $P$ .

To overcome the thermal limitations, discussed above, the pulse pumping of a plasmon resonator can be used. We consider step-like approximation for temporal number of plasmons profile with duration  $\tau_p$ , which is valid if  $\tau_p$  is greater than the establishing time of the plasmon oscillations  $Q/\omega \sim 10 \text{ fs}$ . Note that the steady-state consideration is admissible if the pulse duration is larger than the thermal equilibration time  $\tau_{ss}$ , which is the time of the thermal diffusion  $\tau_{ss} \sim C_{\text{NP}}/(4\pi a^2 h_{\text{NP}}) \sim 0.5 \text{ ns}$ , where  $C_{\text{NP}} \sim 60 \text{ eV/K}$  is the heat capacity of the gold NP of the radius  $a = 10 \text{ nm}$ .

Consider the case of short pulses with  $\tau_p \ll \tau_{ss}$ . The power loss  $P_{\text{heat}}$  is absorbed first by electrons inside the NP. Then the heat is transmitted to the lattice during the electron-phonon interaction time  $\tau_{ep}$ , which is responsible for the equilibration of electrons and lattice temperatures and could be estimated as  $\tau_{ep} \sim 3 \text{ ps}$  for the gold NP [26]. We consider short pulses with the duration  $\tau_p \ll \tau_{ep}$ , since the pulses allow to achieve the highest plasmon population number. At the timescale, electron system of the NP is uncoupled from the metal

lattice and dielectric environment, which hold their initial temperature  $T_0$ .

The total energy stored in the electronic system by the end of the pulse consists of the chaotic contribution of the decayed plasmons and the coherent plasmonic oscillation,  $W = n\hbar\omega\tau_p\gamma_{\text{heat}}(T_0) + n\hbar\omega$ . The energy, accumulated in the electronic system, redistributes between the electrons and metal lattice within the next several  $\tau_{ep}$ . For example, the melting time of a gold nanorod saturates at  $\sim 30 \text{ ps}$  [27] when the laser power increases. The stay-solid condition then reads

$$W \leq C_{\text{NP}}(T_{\text{melt}} - T_0) [+M], \quad (5)$$

where term in the square brackets is the full fusion heat of the NP and should be included if the full melting occurs. Note, that the possible excitation of high-order dark modes due to nonlinear processes [28] does not affect the heating kinetics, because multipole plasmon life-time  $1/\gamma_{\text{heat}} \ll \tau_{ep}$  [11].

Fig. 2 shows the change of temperature for the NP on the  $\tau_p-n$  plane. The partial melting condition corresponds to the area between dashed lines. Large number of quanta  $\sim 10^3$  is not forbidden in the short-pulsed regime, at least due to the thermal limitations. Maximum possible repetition rate can be estimated as the inverse equilibration time  $\tau_{ss}^{-1} \sim 1 \text{ GHz}$ .

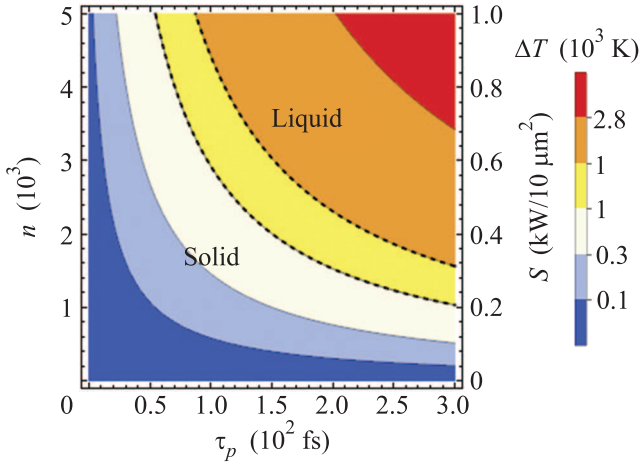


Fig. 2. The temperature change of the NP for its plasmon population during the pulse versus the pulse duration. The area between dashed lines denotes the partial melting region. Right axis shows corresponding power of the driving laser beam. The parameters are as for the Fig. 1, with the standard thermal constants of gold [20]

Anomalous large electric field in NP, which contains finite number of the plasmons, results in appreciable ponderomotive force [29], which can pose a threat of the mechanical damage of the NP. To estimate the influence of this force we consider the NP placed inside liquid or gaseous medium, which does not prevent the deformation of the particle. If the temperature of NP changes insignificantly over period of plasmonic oscillations, i.e.  $n \ll C_{NP}T/(2\pi\hbar\gamma_{heat}) \sim 2.2 \cdot 10^4$ , than the NP can be treated to be in thermal and mechanical equilibrium. Electric force density is  $\mathbf{f} = (\varepsilon - 1)\overline{\nabla E^2}/8\pi$ , where  $\mathbf{E}$  is the electric field, overline stands for time averaging and  $\varepsilon$  is the local dielectric permittivity. Here we adopted the simplest model, when the dielectric susceptibility  $\varepsilon - 1$  is proportional to total density of the medium and there is no influence on the susceptibility from the shear deformations, i.e.  $\rho d\varepsilon/d\rho = \varepsilon - 1$ .

In the case of NP with the most-used dipole mode, the electric force per unit area acting on the boundary between NP and dielectric environment at poles is given by

$$F_p = \frac{(\varepsilon_d + \varepsilon_m - 2\varepsilon_d\varepsilon_m)(\varepsilon_d - \varepsilon_m)}{8\pi\varepsilon_d^2} \overline{\mathbf{E}_0^2}, \quad (6)$$

and the force is zero at the equator, where  $\mathbf{E}_0$  is the electric field inside the nanoparticle. Here we assumed that the particle size is less than skin depth, and therefore, the electric field inside the NP is uniform for a dipole mode. The forces compel the NP to elongate along the dipole direction. The electric field  $\mathbf{E}_0$  can be expressed through the number of plasmons,  $\overline{\mathbf{E}_0^2} = -4\pi n \hbar \omega / (\varepsilon_m a^3)$ . The resonance condition on spher-

ical nanoparticle is  $2\varepsilon_d + \varepsilon_m = 0$ . Setting  $\hbar\omega = 1.9$  eV and  $a = 10$  nm, one can obtain  $F_p \approx n \times 10^6$  Pa. For number  $n \sim 10^2$  of plasmons, this value is about the initial yield stress of the nano-sized gold [30]. However, under the picosecond loads metals go to the plastic state at stresses 10–30 times higher than in the static case [31, 32]. Thus at the short-pulsed regime of excitation the existence of several thousands of plasmon quanta is admissible. Note that the elastic properties of gold are also known to depend strongly on temperature [33]. Simultaneous considering of both the plasmon-induced ponderomotive stress and heating at picosecond timescale may improve the above estimations significantly.

Temperature dependence of the plasmon decay rate in metal is shown to play a crucial role in the heat processes occurring in the plasmonic nanosystems. Resulting nonlinearities lead to the finite number (around unity) of plasmon quanta needed to melt the nanoparticle in CW-regime for real experimental setups. However, the pulsed operation regime allows one to populate the NP with large number of plasmons on the femtosecond timescale. On the other hand, population of the plasmons in the NP is restricted from above by the ponderomotive forces. In the pulsed mode these forces may be large enough to damage the nanosystem. There is still lack of the experimental data for the thermal and strength phenomena in nanoplasmatics; we hope that this paper will motivate further research in that direction.

Authors would like to acknowledge very useful discussions with E. E. Narimanov and N. A. Inogamov. This work was supported by grant RFFI 12-02-01365-a.

1. D. J. Bergman and M. I. Stockman, Phys. Rev. Lett. **90**, 027402 (2003).
2. A. Sarychev, G. Shvets, and V. Shalaev, Phys. Rev. E **73**, 036609 (2006).
3. A. Sarychev and G. Tartakovsky, Phys. Rev. B **75**, 1 (2007).
4. R. F. Oulton, V. J. Sorger, T. Zentgraf, R.-M. Ma, C. Gladden, L. Dai, G. Bartal, and X. Zhang, Nature **461**, 629 (2009).
5. M. Noginov, G. Zhu, A. M. Belgrave, R. Bakker, V. M. Shalaev, E. E. Narimanov, S. Stout, E. Herz, T. Sutee-wong, and U. Wiesner, Nature **460**, 1110 (2009).
6. S. Xiao, V. P. Drachev, A. V. Kildishev, X. Ni, U. K. Chettiar, H.-K. Yuan, and V. M. Shalaev, Nature **466**, 735 (2010).
7. D. K. Gramotnev and S. I. Bozhevolnyi, Nat. Photonics **4**, 83 (2010).
8. A. Brolo, Nat. Photonics **6**, 709 (2012).

9. R. F. Oulton, Mater. Today **15**, 26 (2012).
10. M. I. Stockman, Opt. Express **19**, 22029 (2011).
11. G. Colas des Francs, S. Derom, R. Vincent, A. Bouhelier, and A. Dereux, Int. J. Optics **2012**, 175162 (2012).
12. J. P. Freedman, J. H. Leach, E. A. Preble, Z. Sitar, R. F. Davis, and J. A. Malen, Scientific Reports **3**, 2963 (2013).
13. G. Chen, Phys. Rev. Lett. **86**, 2297 (2001).
14. J. C. Duda, C.-Y.P. Yang, B. M. Foley, R. Cheaito, D. L. Medlin, R. E. Jones, and P. E. Hopkins, Appl. Phys. Lett. **102**, 081902 (2013).
15. O. Neumann, A. S. Urban, J. Day, S. Lal, P. Nordlander, and N. J. Halas, ACS Nano **7**, 42 (2013).
16. M. Liu, M. Pelton, and P. Guyot-Sionnest, Phys. Rev. B **79**, 035418 (2009).
17. J.-S. G. Bouillard, W. Dickson, D. P. O'Connor, G. A. Wurtz, and A. V. Zayats, Nano Lett. **12**, 1561 (2012).
18. O. Yeshchenko, I. Bondarchuk, V. Gurin, I. Dmitruk, and A. V. Kotko, Surf. Sci. **608**, 275 (2013).
19. P. Johnson and R. Christy, Phys. Rev. B **6**, 4370 (1972).
20. T. Castro, R. Reifenberger, E. Choi, and R. Andres, Phys. Rev. B **42**, 8548 (1990).
21. O. A. Yeshchenko, I. M. Dmitruk, A. A. Alexeenko, A. V. Kotko, J. Verdal, and A. O. Pinchuk, Plasmonics **7**, 685 (2012).
22. P. Jund and R. Jullien, Phys. Rev. B **59**, 13707 (1999).
23. Y.-G. Yoon, R. Car, D. Srolovitz, and S. Scandolo, Phys. Rev. B **70**, 012302 (2004).
24. Y. Martynenko and L. Ognev, Tech. Phys. **50**, 1522 (2005).
25. L. Landau and E. Lifshits, *Statistical Physics*, p. 1, 3rd ed., Pergamon, Oxford (1980).
26. S. Link, C. Burda, M. Mohamed, B. Nikoobakht, and M. El-Sayed, Phys. Rev. B **61**, 6086 (2000).
27. S. Link, C. Burda, B. Nikoobakht, and M. El-Sayed, Chem. Phys. Lett. **315**, 12 (1999).
28. D. Östling, P. Stampfli, and K. H. Bennemann, Zeit. für Phys. D **28**, 169 (1993).
29. L. Landau and E. Lifshits, *Electrodynamics of continuous media*, 2nd ed., Pergamon, Oxford (1984).
30. D. Lee, X. Wei, M. Zhao, X. Chen, S. C. Jun, J. Hone, and J. W. Kysar, Model. Simul. Mater. Sci. Eng. **15**, 181 (2007).
31. B. J. Demaske, V. V. Zhakhovsky, N. A. Inogamov, and I. I. Oleynik, Phys. Rev. B **87**, 054109 (2013).
32. V. H. Whitley, S. D. McGrane, D. E. Eakins, C. A. Bolme, D. S. Moore, and J. F. Bingert, J. Appl. Phys. **109**, 013505 (2011).
33. L. Condra, J. Svitak, and A. Pense, IEEE Transactions on Parts, Hybrids, and Packaging **11**, 290 (1975).